Journal of Geoscience and Environment Protection, 2026, 14(5), 244-264
https://www.scirp.org/journal/gep
ISSN Online: 2327-4344
ISSN Print: 2327-4336

Synthesis and Characterization of Porous Materials from Paleocene-Ypresian Clay Minerals Activated with Na_2CO_3 from Oued Abiod (Central Tunisia)

Mohamed Mosbahi[1*], Ali Tlili[2], Fakher Jamoussi[1]

[1]CERTE, Laboratoire de Georessources, Technopôle de Borj Cedria, Soliman, Tunisie
[2]Laboratoire GEOGLOB (code LR13ES23), Département des Sciences de la Terre, Faculté des Sciences, Université de Sfax, Route Sokra Km, Sfax, Tunisia
Email: *mohamedmosbahi1@gmail.com

How to cite this paper: Mosbahi, M., Tlili, A., & Jamoussi, F. (2026). Synthesis and Characterization of Porous Materials from Paleocene-Ypresian Clay Minerals Activated with Na_2CO_3 from Oued Abiod (Central Tunisia). *Journal of Geoscience and Environment Protection, 14,* 244-264.
https://doi.org/10.4236/gep.2026.145015

Received: April 23, 2026
Accepted: May 26, 2026
Published: May 29, 2026

Abstract

Paleocene-Ypresian clay minerals of Meknassy region in the central Tunisia are characterized with mineralogical variety: Smectite, illite, kaolinite, sepiolite and palygorskite. This mineralogical diversity encourages the valorization of these clays in several industrial fields. In this work, the basic activation of the studied clay with Na_2CO_3 (5%) and its leads to transformation into microporous and mesoporous materials are a potential approach to integrate advantages of Na-smectite and different material structures for desirable properties and applications. Indeed, the basic activation of these clays increases the specific surface, augmenting from 30.41 to 150 m^2/g and causing the ionic exchanges Na-Ca, Na-K and Mg-Al between the Ca-smectitic, the kaolinite, the palygorskite, the sepiolite, the dolomites and the sodium carbonate, resulting in the formation of microporous and mesoporous materials. All the samples collected from the Oued Abiod section, before and after activation, were the object of a mineralogical characterization by XRD and SEM, a chemical characterization by X-ray fluorescence, a physical characterization (pH, IR) and Particle size distribution by a Mastersizer S laser particle size analyzer. The SEM observation strongly reveals the transformation of the activated natural clays of the HOA3 sample, in an alkaline environment where pH = 10, into tubular-shaped materials of important porosity and regular and irregular morphology.

Keywords

Paleocene-Ypresian Clays Minerals, Activation, Na_2CO_3, Microporous and

Mesoporous Materials

1. Introduction

Clay minerals (Smectite, illite, kaolinite, sepiolite and palygorskite) are non-toxic natural materials. These materials are characterized by an important specific surface which confers them a big capacity of absorption and adsorption. Their industrial use is vast: The purification and clarification of vegetable oil (Mosbahi, 2017; Issaoui et al., 2021), adsorbants, decontaminants (Sdiri et al., 2016), Bleaching agents, catalysts, catalyst supports, oil drilling mud, animal feed additives, cosmetic and pharmaceutical products (Gamoudi & Srasra, 2017-2018; Sylla et al., 2017), and inorganic hybrids. Once activated by an acid or by a base, these materials show a new structure and a morphology and their specific surface increases considerably.

The activated clay by Na_2CO_3 is used as mud of drilling and for the clarification of soybean oil (Mosbahi et al., 2017). The choice of the activation with Na_2CO_3 of Paleocene-Ypresian clays has a wide industrial use, because it is less expensive, and less polluting than acids. Also, clays activated with Na_2CO_3 can be transformed into zeolites (Mosbahi, 2017). According to Sheela Evangeline et al. (2009), the increase of the porosity and the maximal reduction of the permeability are noticed when the calcic bentonite is treated with Na_2CO_3. This work is the continuity of the research by Mosbahi (2017) concerning the valorization of raw and activated clay minerals of the Meknassy-Mezzouna basin in the central Tunisia.

The innovative aspect of the present study is the synthesis and characterization of porous materials after basic activation of Paleocene-Ypresian clay minerals. Three samples collected from the Oued Abiod section (HOA1, HOA2 and HOA3), expose a heterogeneous mineralogical procession which changes from one level to another. Three samples collected from the Oued Abiod section (HOA1, HOA2 and HOA3) exhibit a heterogeneous mineralogical assemblage, varying between stratigraphic levels. The study of these three clays of different mineralogical composition allows us to understand their structural and morphological behavior in an alkaline environment. These raw natural clays are selected according to the richness in smectite as well as the presence of fibrous clays (palygorskite and sepiolite). Their specific surface varies from 4 to 30.41 m^2/g.

2. Location, Geological Setting and Lithological Description

The studied area is located in the southern part of central Tunisia (**Figure 1**). It is separated from the Tunisian trench (or groove) to the north by the large NE-SW Zaghouan flexure and from the Saharan craton to the south by the South-Atlasic fault of Gafsa (which runs NW-SE to WNW-ESE) (Soyer, 1987). Central-eastern Tunisia and the Pelagian Platform are affected by a system of several-kilometer-

long faults oriented NW-SE to NNW-SSE: They are the faults of Gafsa, Kasserine and Sbiba-Kalaa Jerda (Boltenhagen, 1981). During the upper Cretaceous, the sedimentation with ascendancy of clay, limestone and dolomite, gives evidence of an environment much deeper than in the Eocene. This period also distinguishes itself by important variations of thicknesses which would be engendered by the major faults affecting the basin. This relation between the tectonics and the sedimentation of the Cretaceous platform was the object of several works (Chihi et al., 1984; Ben Ayed, 1986; Mosbahi et al., 2014).

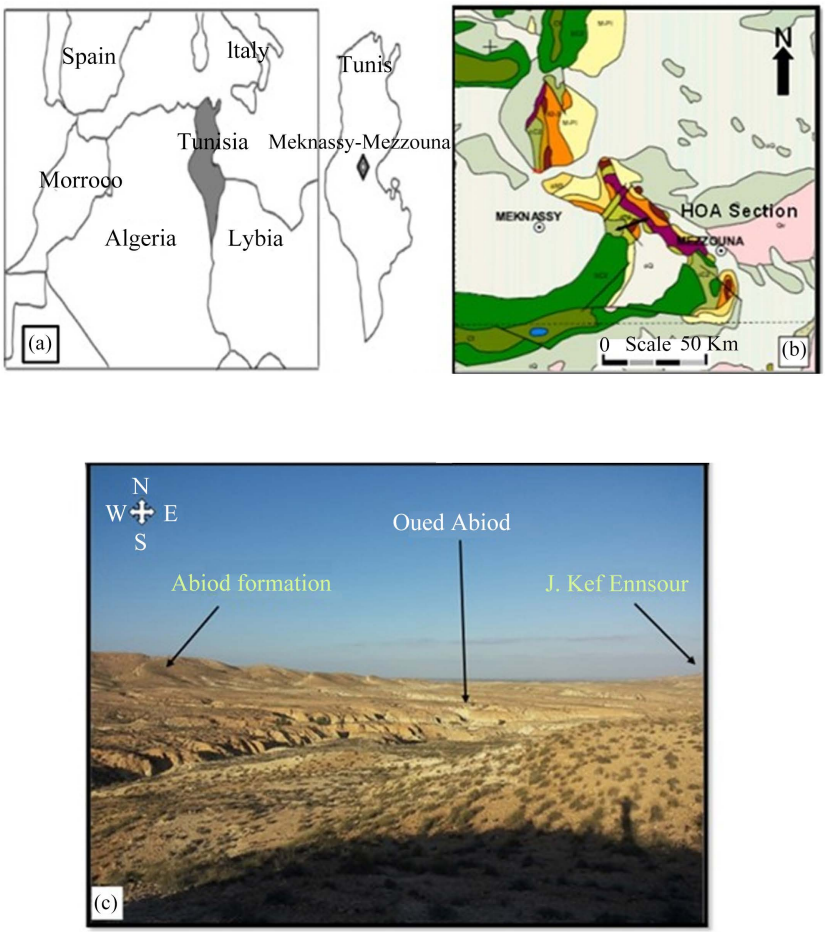

Figure 1. (a) Geologic outcrops at Jebel Meheri El Jebbes showing position of lithological section and (b) Location of the Meknassy region, Centerwestern Tunisia.

The studied section was raised at the level of Oued Abiod (**Figure 1(c)** and **Figure 2**). This site is situated approximately 6 kilometers in the ESE of the city of Meknassy, in the North of Jebel Bou Douaou. The section shows from the bottom up the following succession (**Figure 2**): Chalky white limestone of the Abiod formation; Quaternary deposit covers clays; Green foliated clay, containing the secondary gypsum; Blackish clay, flowing in centimetric and decimetric foliated balls rich in pyrite; Greenish clay in yellowish flow of centimetric and decametric and sometimes foliated; small phosphated layers and; a gypseous layer.

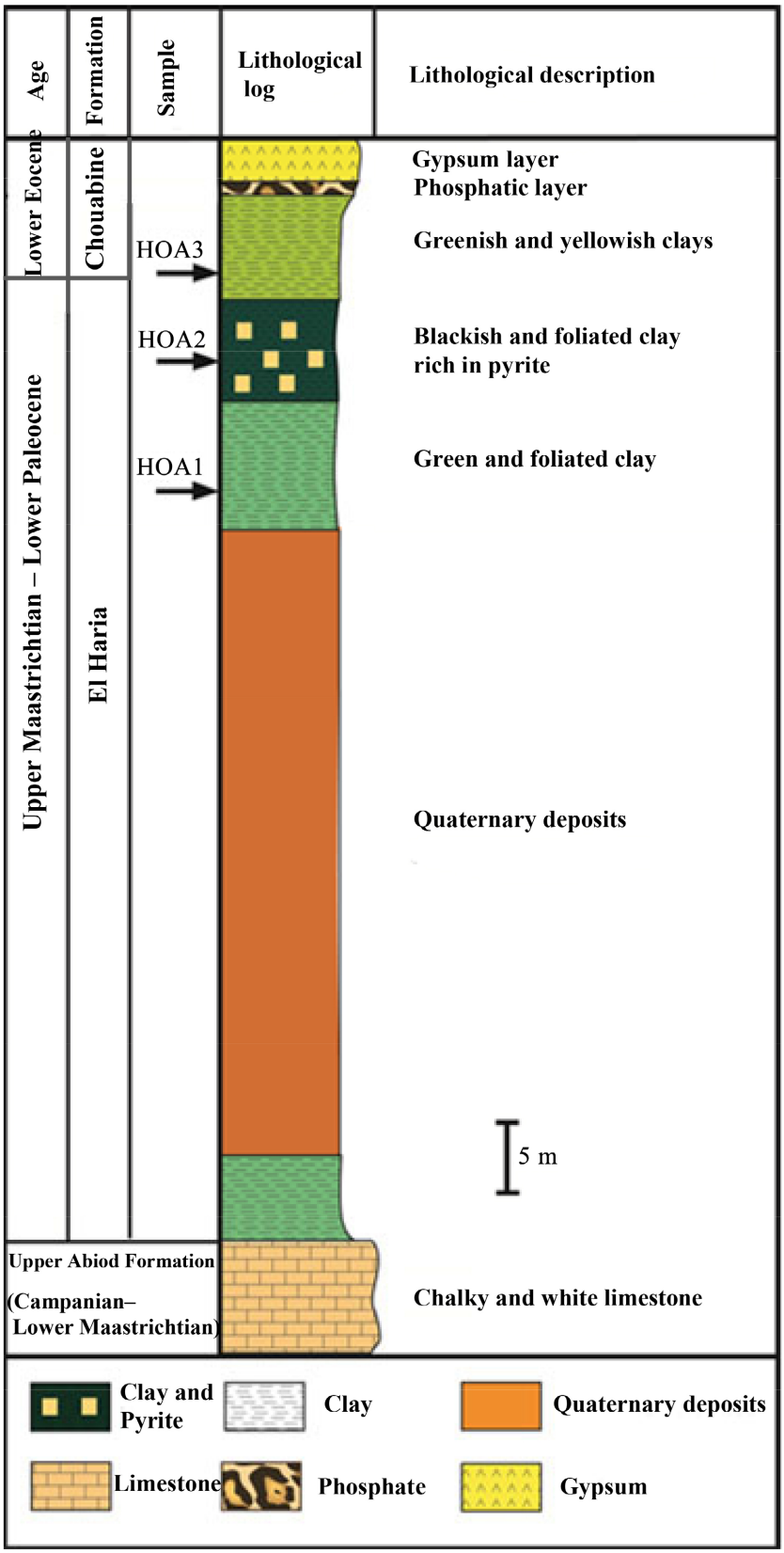

Figure 2. HOA lithological section along the Paleocene-Ypresian of Oued Abiod outcrops at the Meknassy region.

3. Materials and Methods

3.1. Materials

Three natural clay samples of different mineralogical procession are collected from the Oued Abiod section. These clays are suspended in water and sieved by a 40 μm sieve to remove impurities, and then dried in an oven at 60˚C. A mixture of 15 g of sieved clay and a quantity of Na_2CO_3 (5%) is soaked in 150 ml with distilled water then put under continuous agitation for an hour. The better results of activation for clays were obtained with 5% of added Na_2CO_3. The selection of 5% Na_2CO_3 at 75˚C as the optimal condition was determined based on experimental results from doctoral research of Mosbahi, 2017. These parameters were optimized as part of this study and are also reported in a previous publication (Mosbahi et al., 2017), where detailed experiments were conducted to validate this condition. For that reason, we present in this work only the results of the activation of clays realized with 5% of basic added in 75˚C during one hour (Mosbahi, 2017; Mosbahi et al., 2017). Raw and treated natural clays are characterized by various analysis techniques: X-ray Diffraction (XRD), specific surface area measurement by nitrogen adsorption at 77 K (BET), X-ray fluorescence (XRF), chemical analysis, pH measurement, and scanning electron microscopy (SEM).

3.2. Methods

3.2.1. Specific Surface Area and Porous Volume

The BET surface analysis and the porosity of the clays (before and after activation) were performed at the "Laboratory of Sorptiometry" using a Quantachrom-Autosorb Specific surface area analyzer. The nitrogen gas sorption method was used at 77 K for specific surface area determination. The pore space volumes were evaluated Barrett-Joyner-Halenda's method, from the adsorption branch. The samples were outgassed at 393 K under a vacuum at 10^{-3} mm Hg for 3.5 h.

3.2.2. Chemical Analysis: X-Ray Fluorescence

The chemical analysis of raw and activated clay of the Oued Abiod section were conducted by X-ray Fluorescence techniques on fused glass pearls using type Oasis 9900, Thermo-Fisher, in the Control and Quality Laboratory at the Gabès Cement Company. The XRF is a rudimentary analysis technique of the sample, representing an excitation of the sample with X-rays when the analyzed material emits secondary X-ray emission, called fluorescence X. From the characteristic X-ray spectra of the sample composition, the elemental composition can be deduced, i.e., the mass concentrations of the elements. The identification of the major elements requires sample preparation in the form of pellets in a transparent lithium tetra borate. The weight loss on ignition was measured by calcination at 1000˚C.

3.2.3. X-Ray Diffraction

The clay fraction was separated from larger particles by decantation and centrifugation (Brindley & Brown, 1980). Such fine fraction was subjected to a series of

analyses. In fact, the X-ray diffraction analyses were carried out on two types of preparations. With respect to the first one, it concerns the diffractograms of oriented preparations, in which the phase identification is based on the diagrams of fine fractions after physico-chemical treatments (normal, glycoled and heated to 550˚C) (Moore & Reynolds, 1997). As for the second type, it relates to the preparation of powder diffractograms of raw and treated clay. The latter presents the set of rays (hkl) of all minerals composing the sample. The estimate of the percentage of each mineral is affected by the integration of the area of the most intense peak (Mosbahi et al., 2014, 2017). All XRD data were collected under the same experimental conditions using an X'pert HighScore plus PANalytical diffractometer. Philips PW type diffractometer PANalytical X Pert Pro MPD (θ - 2θ) system, equipped with a copper anticathode, was used CuKα radiation source under 40 kV/40mA and an angular range of 3˚ - 70˚ 2θ for bulk rocks and 3˚ - 30˚ 2θ for fine fraction, a step size of 0.017˚2θ, and a counting time of 10 s/step to determine mineral composition.

3.2.4. SEM Analysis

The morphology of raw clays treated by Na_2CO_3 samples (HOA1, HOA2 and HOA3) of the Oued Abiod section was observed by an electronic microscope of the type HITACHI SC-2500's sweeping. The principle of this technique is based on the strong interaction between the spread emitted and retro secondary electrons which allow to reconstitute the image of the object. The working tensions are generally between 10 and 30 kV, which allows to have a swelling that can go to 30.000 times. The set is silvered by a gold layer to make it conductive before the observation.

3.2.5. PH Meter

The pH of six samples of raw and activated clays is measured by a pH measure, Typifies NeoMet 200 L in the microbiological laboratory of the Faculty of Science of Sfax.

3.2.6. Micro-Grading Analysis by Diffraction Laser

The particle size distribution of the raw clays and those activated with Na_2CO_3 was analyzed using laser diffraction. This analysis was carried out using a wet method at the Tunisian Chemical Group Factory in Gabès. The particle size distribution was measured with a Mastersizer S laser particle size analyzer.

4. Results

4.1. Determination of BET Specific Surface Area and Pore Volume

Table 1 shows that the specific surface by BET of raw clays varies from 4 to 30.41 m^2/g (HOA1: SBET = 4 m^2/g; HOA2: SBET = 11 m^2/g; HOA3: SBET = 30.41 m^2/g). After basic activation of these three clays, the specific surface increases in a significant way. Better results were obtained at the top of this section (HOA3: SBET = 150 m^2/g).

Table 1. Specific Surface (BET) of clay samples before and after activation.

Sample	Specific Surface BET (m^2/g)		Porosity	
	Raw clay	Activated clay	Raw clay	Activated clay
HOA3	30.41	150	17.2	80.14
HOA2	4.94	11	2.8	6.42
HOA1	4	7	2.27	3.97

4.2. Chemical Characterization of Raw and Activated Clays

Table 2 shows that the chemical composition changes upon activation, with CaO decreasing from 6% to 3.8% and Na_2O increasing from 1.2% to 7.9%. This is due to the replacement of Ca^{2+} ions by Na^+ ions. Furthermore, the increase in Na_2O is more pronounced than the decrease in CaO. Other divalent ions, such as Mg^{2+} and Fe^{2+} (with MgO and Fe_2O_3 decreasing from 5.22% to 1.86% and from 4.34% to 2.7%, respectively), as well as trivalent ions (Al^{3+} and Fe^{3+}) present in the samples, are also partially replaced by Na^+. These substitutions, promoted by Na_2CO_3, lead to the formation of sodic smectite and hydrated aluminosilicate microporous materials, such as zeolites. The synthesized products exhibit high porosity and lower permeability.

Table 2. Results of the chemical analyses of sample HOA3 from Oued Abiod: raw and activated.

Oxyde (%)	Raw clay (HOA3)	Activated clay (HOA3)
SiO_2	43.71	51.20
Al_2O_3	12.43	12.11
Fe_2O_3	4.34	2.7
MgO	5.22	1.86
K_2O	2.05	1.03
Na_2O	1.21	7.88
CaO	6.01	3.85
SO_3	0.49	0.3
P_2O_5	1.75	1
LOI	24	17.07
Total %	100	99

4.3. Mineralogical Characterization and Morphology of Studied Clay (before and after Treatment)

4.3.1. DRX Analysis

The mineralogical analysis by XRD of the HOA1 sample before basic activation shows a clay procession prevailed by the smectite (80%) to which the kaolinite is joined (Figure 3 and Figure 4).

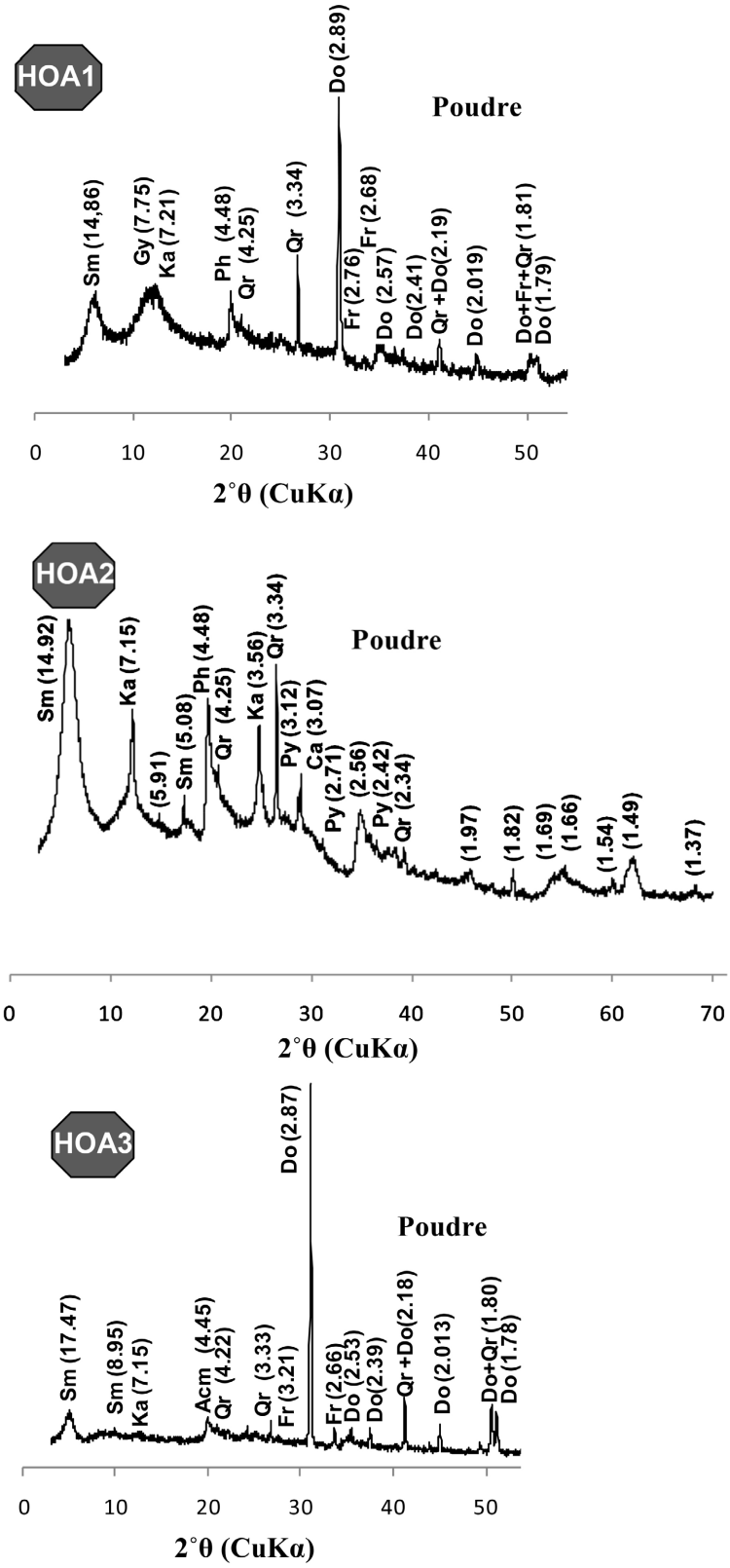

Figure 3. XRD patterns (CuKα radiation) of the raw clay of the HOA1, HOA2 and HOA3 samples (Oued Abiod). (Sm) smectite; (Ka) Kaolinite; (Acm) all clay minerals; (Ca) calcite; (Do) dolomite; (Qr) quartz; (Fr) francolite; (Gy) gypsum.

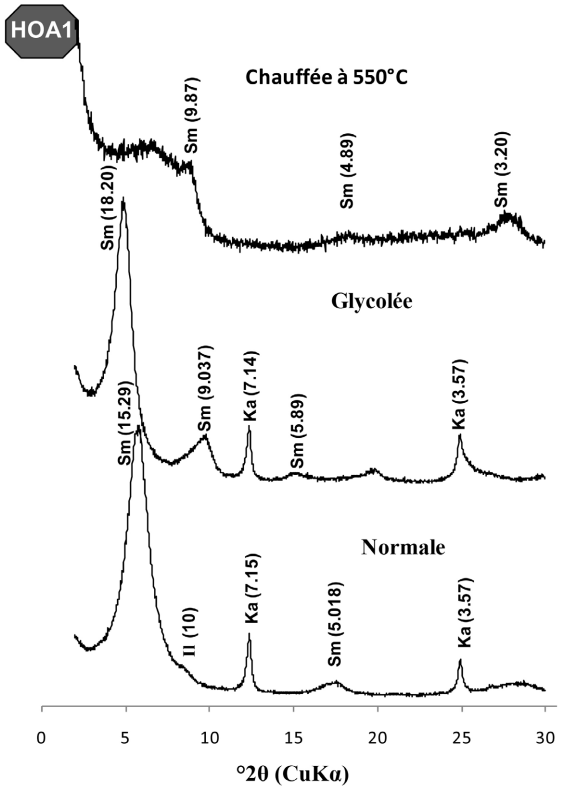
HOA1
Chauffée à 550°C
Sm (9.87)
Sm (4.89)
Sm (3.20)
Sm (18.20)
Glycolée
Sm (9.037)
Ka (7.14)
Sm (5.89)
Ka (3.57)
Sm (15.29)
Normale
Ka (7.15)
Il (10)
Sm (5.018)
Ka (3.57)
0
5
10
15
20
25
30
°2θ (CuKα)

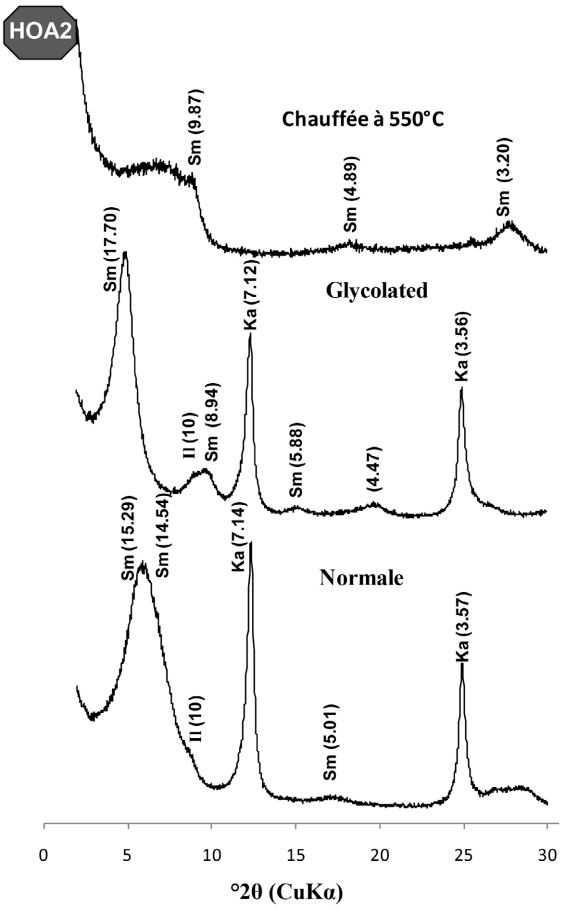
HOA2
Chauffée à 550°C
Sm (9.87)
Sm (4.89)
Sm (3.20)
Sm (17.70)
Glycolated
Ka (7.12)
Ka (3.56)
Il (10)
Sm (8.94)
Sm (5.88)
(4.47)
Sm (15.29)
Sm (14.54)
Ka (7.14)
Normale
Ka (3.57)
Il (10)
Sm (5.01)
0
5
10
15
20
25
30
°2θ (CuKα)

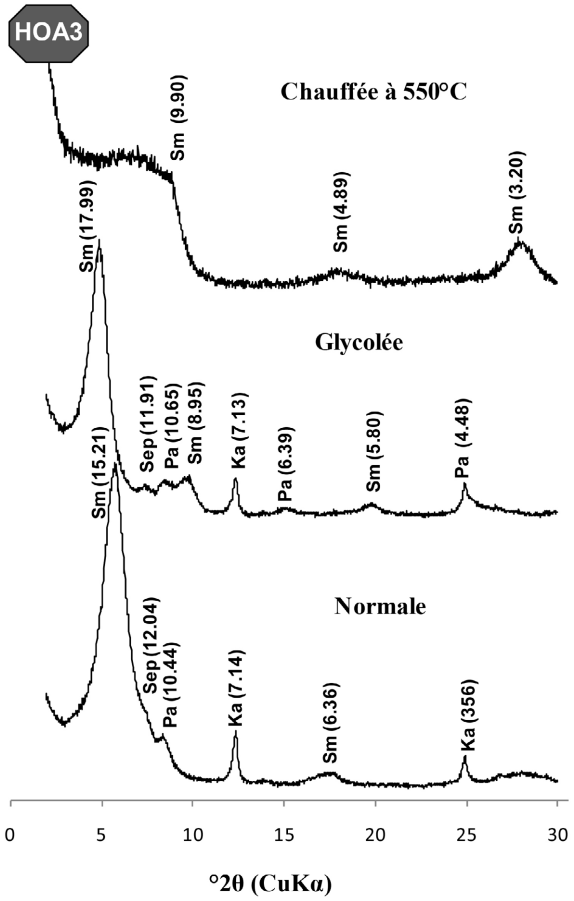

Figure 4. XRD patterns (CuKα radiation) of three oriented clay fractions of the HOA1, HOA2 and HOA3 samples (Oued Abiod) (Sm: smectite; Sep: sepiolite; Pa: palygorskite, Ka: kaolinite, Il: illite).

The non-clay procession is composed of dolomite, quartz and gypsum. After basic activation by Na_2CO_3 (5%) at 75˚C, the studied clay shows a decrease of the intensity of the peaks of the smectite and the kaolinite, the appearance of a low peak of feldspar characterized by its main ray in 3.19 Å, the persistence of secondary mineral peaks (quartz and dolomite) and the disappearance of the gypsum after this basic activation by Na_2CO_3.

The calcic or rather magnesian smectite before activation, characterized by its main ray in 15.71 Å, becomes a sodic smectite after activation, characterized by a main ray 12.37 Å (Figure 5(a)).

In the middle part of the summit of Oued Abiod section (Figure 3), the diffractogramme of the HOA2 sample presents intense peaks of smectite and kaolinite before treatment, while the illite appears track there. The quartz shows a slightly intense peak against a low calcite peak. All these minerals persist after basic activation at 75˚C (Figure 5(b)), but with lower proportions than at the beginning. The appearance of the intense peaks (12.47 - 3.19 - 3.06 Å) after this activation by Na_2CO_3 (Figure 5(b)) could be explained by the beginning of zeolitisation of the activated sample HOA2 confirmed by the observation by SEM.

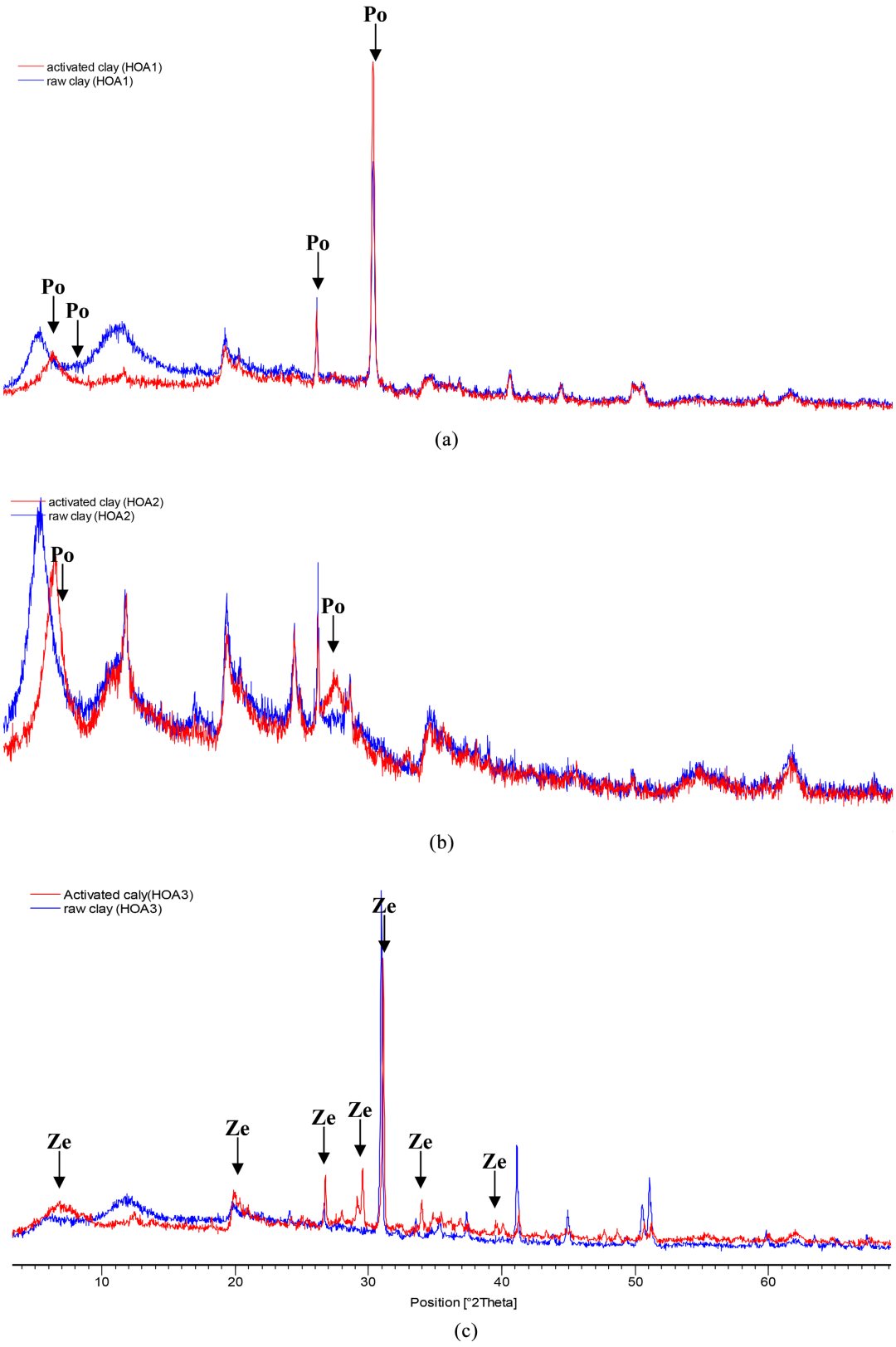

Figure 5. XRD patterns (CuKα radiation) of the clay (<40 µm) (raw and activated with 5% Na_2CO_3 at 75˚C for one hour) of HOA samples: (a) HOA1; (b) HOA2; (c) HOA3. (Sm) smectite; (Po) porous materials; (Ze) zeolite; (Pa) palygorskite; (Sep) sepiolite; (Ka) kaolinite; (Acm) all clay minerals; (Ca) calcite; (Do) dolomite; (Qr) quartz.

At the upper part of this section, the HOA3 sample (Figure 4) shows a high percentage of smectite (80%), a low rate of kaolinite and tracks of illite, palygorskite and sepiolite. The non-clay procession of this sample presents a high percentage of dolomite, a small proportion in quartz and francolite (Figure 3). After basic attack by solid Na_2CO_3, all the peaks of clay and non-clay minerals change intensity (Figure 5). The confrontation of the obtained results by the X-rays and those obtained by SEM confirm that this activated clay in the best already mentioned conditions was transformed to mesoporous materials or zeolite.

4.3.2. SEM Observations

1) Before treatment

The HOA1 sample selected from Oued Abiod section, allows to underline an abundance of rhombohedral dolomite crystals. These dolomites are well crystallized and mixed in a clayey matrix (Figure 6(a) and Figure 6(b)). The photomicrographs (b), detail of the photomicrographs (a), expose a richness in foliated clay of smectite nature. These minerals, characterized by their main reflection 15.29 Å, are detected in the normal aggregate.

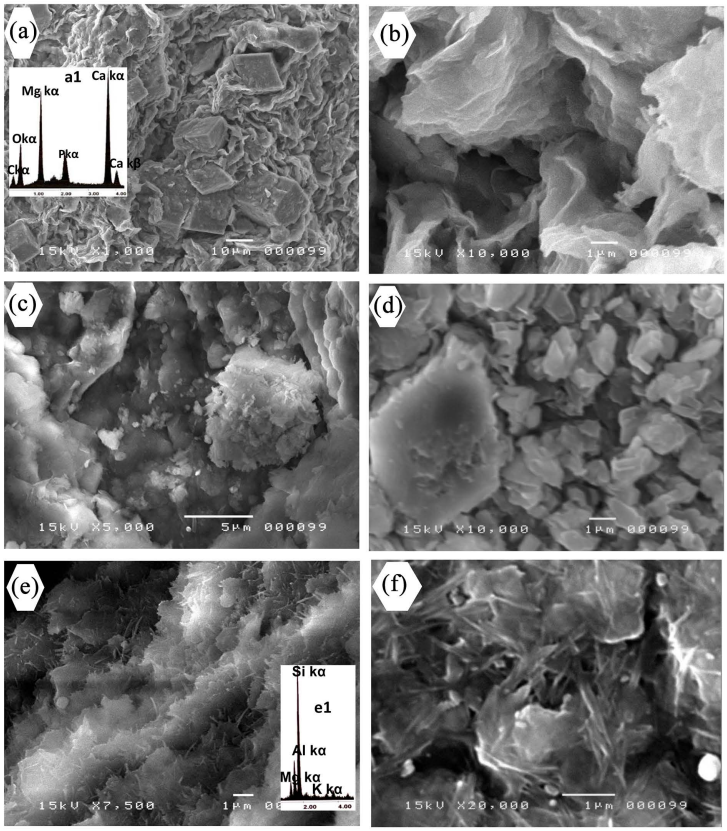

Figure 6. ((a), (b)) HOA1, (a) an abundance of rhombohedral dolomite in a clay matrix; (b) layered texture showing a richness in smectite. (a1) Their EDX analysis reveals Ca, Mg, Si, and Al. ((c), (d)) HOA2, (c) flaky and platelet-like clay; (d) abundance of kaolinite in the form of platelets. ((e), (f)) HOA3, (e) fibrous clays interspersed with a cotton-like texture; (f) fibrous clays (palygorskite and sepiolite) in the form of spines. (e1) EDX reveals Mg, Si and Al.

The sample HOA2, taken in the middle of the summit part (Figure 6(c) and Figure 6(d)), expresses a richness in smectite and kaolinite mixed with the pyrite.

A fragment of the sample HOA3 shows the abundance of rhombohedral crystals of dolomite scattered in a clayey matrix (Figure 6(e) and Figure 6(f)), and which are sometimes altered. The microanalysis X confirms the dolomitic nature with the presence of the peaks of the Ca and Mg. These crystals are surrounded by smectites (Figure 6(e)). Frequent fibrous clays show a thorny aspect and a lifeless appearance. These fibers are associated with a foliated matrix (Figure 6(f)). These results are confirmed by XRD (Figure 4).

2) After treatment

The SEM observation of the morphology of clays from the HOA1 sample activated with 5% Na_2CO_3 at 75˚C reveals the significant dissolution of smectite layers, particularly rhombohedral dolomite (Figure 7(a) and Figure 7(b)). It is observed that the basic activation leads to the partial dissolution of phyllosilicates and attacks the dolomite crystals (Figure 7(a) and Figure 7(b)). Considering that dolomitization involves the transformation of calcite to dolomite through the circulation of fluids rich in magnesium salts, the dissolution of dolomite in clays activated under the described conditions does not result in the formation of calcite. Instead, it promotes zeolitization and the formation of smectite-Na (Figure 7(b)).

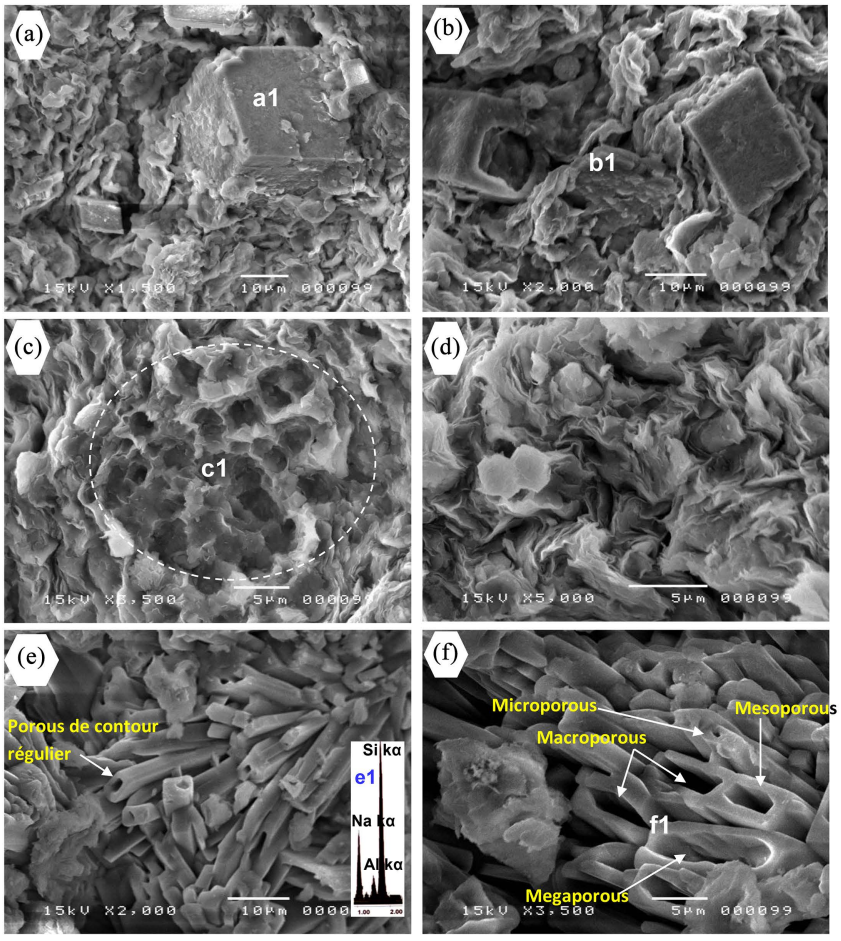

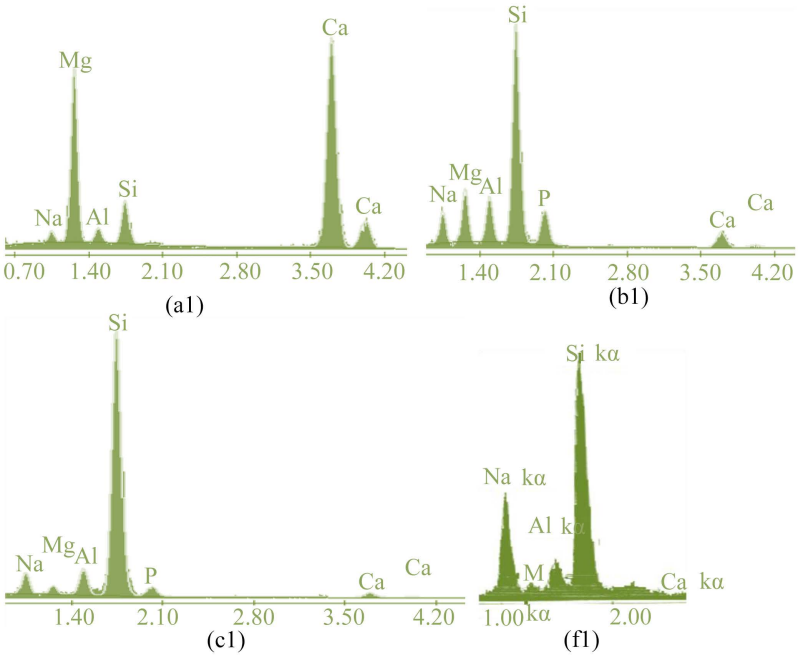

Figure 7. Scanning Electron Microscopy (SEM) observation of HOA samples activated by Na_2CO_3. ((a), (b)) HOA1, showing significant dissolution of smectite sheets (a); dolomite undergoing dissolution ((a), (b)); perforated and altered dolomite disseminated within the Na-smectite (b). The X-ray microanalysis of a dolomite rhombohedron in micrograph (b) shows very intense peaks of Mg and Ca. ((c), (d)) HOA2, reveals a porous texture of zeolites in the form of a sponge, with EDX analysis (a) revealing the presence of Si, Al, Na; (c) smectite sheets and kaolinite platelets in a smectitic matrix. ((e), (f)) HOA3 shows an amalgam of crystals in the form of aggregates and tubular structures; (e) zeolites in the form of tubules crossed by pseudohexagonal tunnels of varying lengths; (f) this micrograph displays several types of porosity (micropores, macropores, mesopores, and macropores) in a new homogeneous phase. X-ray microanalysis reveals two intense peaks of Si and Na, a small peak of Al, and traces of Mg and Ca.

The HOA2 sample after treatment exhibits a porous, sponge-like texture, with calcite crystals that are partially or fully altered, and sometimes dissolved. It also shows a clay with a foliated and porous appearance, as well as plates of kaolinite. The structures observed after this basic activation, as seen in micrograph (c) of Figure 7, resemble honeycomb patterns formed by pores, cages, and channels. These are zeolites, which were identified by XRD (Figure 7(c) and Figure 7(d)). The X-ray microanalysis of the micrographs (c) reveals the characteristic energy lines of Si, Al, and Na. This zeolitic structure imparts specific properties, including those of a molecular sieve and a selective catalyst.

The SEM observation of the activated HOA3 clay sample reveals the presence of an almost homogeneous crystalline phase, corresponding to a zeolite (Figure 7(e) and Figure 7(f)). This crystallization is associated with the simultaneous presence of clay minerals (smectite, palygorskite, and sepiolite) and non-clay minerals such as dolomite and quartz in an alkaline environment with a pH of 10. Elongated tubular crystals of varying size and shape indicate the presence of one or more varieties of zeolite (Figure 7(e) and Figure 7(f)).

4.4. PH Measurement

The pH of the studied clays before activation varies from 7.32 to 8.31 (Table 3). Clays of samples HOA3 before treatment are slightly basic (pH = 7.31); after activation by the base Na_2CO_3 in the conditions of activation (5% Na_2CO_3, 75˚C, 1 hour), the pH of these clays mounts to 10 (Table 3). These clays with ascendancy of smectite and contain the palygorskite, the sepiolite and the dolomite, are transformed into zeolite (Mosbahi et al., 2017). On the contrary, sample HOA1 and HOA2 is basic before activation, their pH is upper to 8 and their mineralogical procession of departure is formed by the smectite, the kaolinite and the calcite. After activation, these clays give sodic smectites rather than zeolites, though the pH reached 10.

Table 3. pH of raw and activated clay by 5% Na_2CO_3 (1 h at 75˚C).

Sample	pH	
	Raw clay	Activated clay by 5% Na_2CO_3 (1 h, 75˚C)
HOA3	7.32	10.46
HOA2	8.22	10.63
HOA1	8.31	10.67

4.5. Granulometry of the Clays from the HOA Section before and after Activation

The particle size distribution of the two samples, HOA1 and HOA2, from the Oued Abiod section is bimodal both before (Figure 8(a1) and Figure 8(a2)) and after activation (Figure 8(a2) and Figure 8(b2)). This can be explained by the mineralogical composition before treatment. The recrystallization of smectite and kaolinite in the presence of calcite is minimal after basic treatment for both HOA1 and HOA2 samples.

The change in particle size distribution of sample HOA3, shifting from a unimodal distribution before activation (Figure 8(c1)) to a bimodal distribution after activation with solid Na_2CO_3 (Figure 8(c2)), can be explained by the redistribution and recrystallization of the composite atoms within the crystal lattice of these smectitic and fibrous clays, in the presence of dolomite and quartz, which are sources of Mg and Si, respectively. This granulometric redistribution in this sample is attributed to the formation of Na-smectite and zeolites. This result is confirmed by mineralogical analyses (XRD and SEM).

5. Discussion

The raw clays from samples HOA1 and HOA2, collected from the Oued Abiod section, date back to the Paleocene. The mineralogical composition of these clays is dominated by smectite and kaolinite, with secondary minerals mainly consisting of quartz and dolomite in sample HOA1 (Table 4). The basic activation of these clays resulted in the formation of sodium-rich smectites and some dolomite, but no zeolite formation was observed (Figure 5(a) and Figure 5(b)).

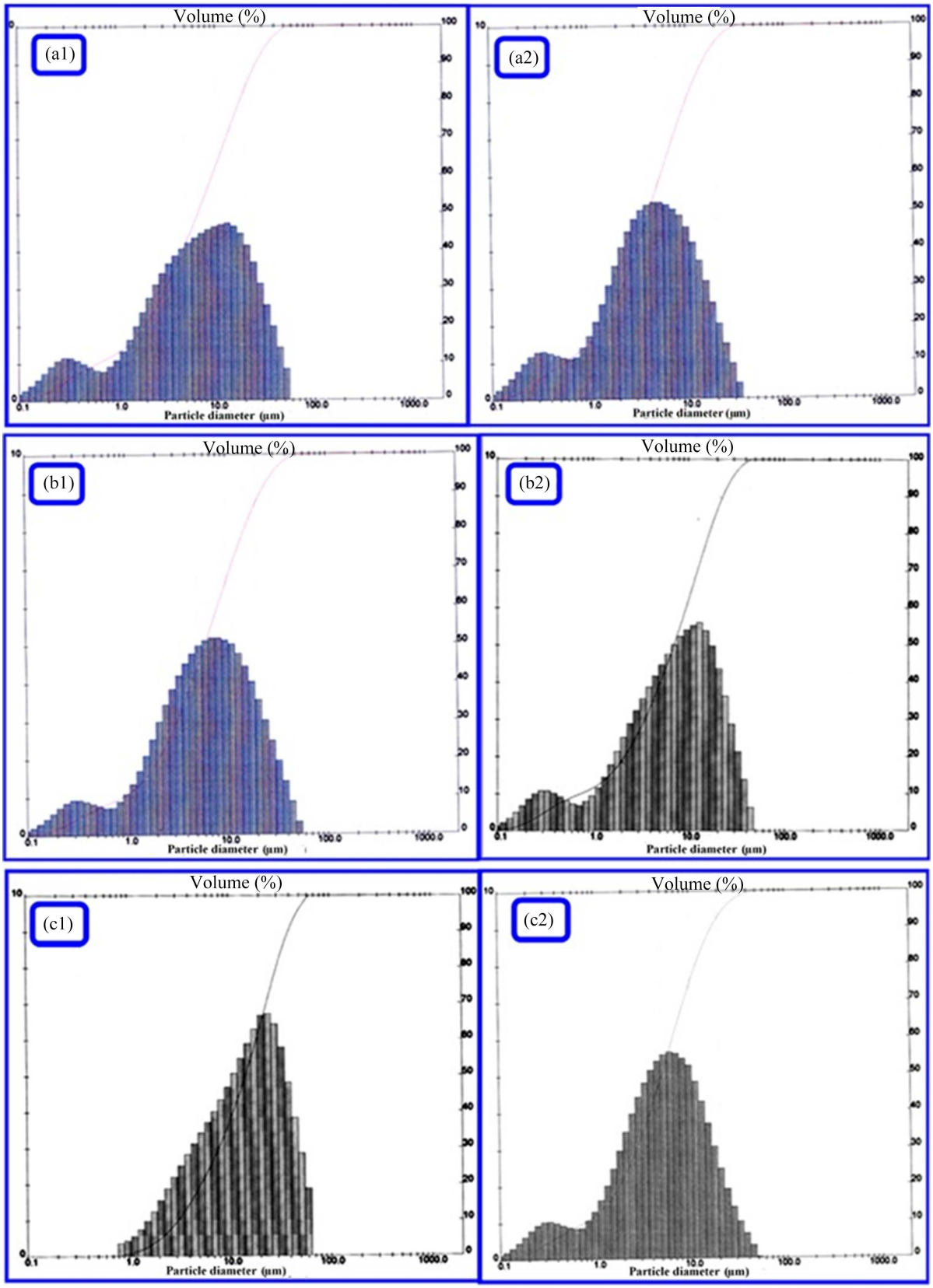

Figure 8. Particle size distribution of raw and activated clays. HOA1 (a): (a1) before activation; (a2) after activation; HOA2 (b): (b1) before activation; (b2) after activation; HOA3 (c): (c1) before activation; (c2) after activation.

Table 4. Mineralogical Composition of studied clays. Sm = smectite; Il = illite; ka = kaolinite; Se = sepiolite; Pa = palygorskite; Gy = gypsum; Ca = calcite; Qr = quartz; Do = dolomite; Fr = francolite; Py = pyrite.

Section	Sample	Mineralogical composition of natural clays (%)										
		Clay minerals					Non-clay minerals					
		Sm	Il	Ka	Se	Pa	Gy	Ca	Qr	Dol	Fr	Py
Oued Abiod	HOA3	58	0	5	2	4	0	0	2	27	2	0
	HOA2	59	1	14	0	0	0	8	13	0	0	5
	HOA1	58	1	6	0	0	20	0	3	9	3	0

X-ray diffraction (XRD) and scanning electron microscope (SEM) analyses of the raw clay from sample HOA2 show that the non-clay minerals present are primarily quartz and pyrite (**Table 4**). After basic activation, the clays of HOA2 displayed a more porous texture, as observed in SEM images (**Figure 5(c)** and **Figure 5(d)**).

In contrast, the clays from sample HOA3 are predominantly composed of smectite (approximately 90%) along with small amounts of palygorskite, sepiolite, kaolinite, dolomite, and quartz (**Table 4** and **Figure 4(e)** and **Figure 4(f)**). After activation, mineralogical transformations were observed, including dissolution, recrystallization, and rearrangement of particles (**Figure 5(e)** and **Figure 5(f)**). SEM and XRD observations show that the activation process significantly improved the crystallization of pre-existing minerals (smectite, sepiolite, palygorskite, quartz), led to the formation of new mineral phases (zeolites and sodium smectite), and caused partial to complete dissolution of the rhombohedral dolomite (**Figure 5(a)** and **Figure 5(b)** and **Figure 5(e)** and **Figure 5(f)**).

The formation of zeolites was particularly pronounced after basic activation at 75˚C, where the zeolites developed at the expense of pre-existing crystals (smectite, sepiolite, palygorskite, dolomite, and quartz). Ionic substitutions within the interlayer space of smectite occurred between sodium (Na) from Na_2CO_3 and the original cations in the smectite structure (Lebedenko & Plée, 1988; Warren, 2000; Yildiz & Calimli, 2002; Gougeon et al., 2003; Sheela Evangeline et al., 2009). Transmission electron microscopy (TEM) analysis confirmed the formation of sodium-rich smectites and zeolites after activation (5% Na_2CO_3, 1 hour, 75˚C) (Mosbahi, 2017; Mosbahi et al., 2017).

This ion-exchange reaction facilitates the activation of low-temperature calcium-rich smectites. Since most Tunisian smectites are calcium-rich and exhibit limited swelling, this sodium activation in an alkaline environment is highly beneficial for activating and enhancing these smectites. It is likely that the replacement of calcium (Ca) and/or potassium (K) by sodium (Na) in the interlayer space of smectite is followed by the substitution of magnesium (Mg) for aluminum (Al). Sheela Evangeline et al. (2009) showed that as the Na content increases in bentonites, the level of calcium decreases, and Na also replaces other cations in the crystal

lattice of the bentonites.

During the basic treatment of these clays, the consumption of magnesium (Mg^{2+}) from the partial or total destruction of dolomite leads to a reduction in its content and the formation of zeolitic phases after activation (**Figure 5**). Therefore, sodium (Na) and carbonate (CO_3) likely originate from both the smectite and the destruction of rhombohedral dolomite. The incorporation of Na into the crystal lattice of smectite facilitates the synthesis of zeolites, particularly LTA ($Na_2Ca_2Al_6Si_9O_{30}{\cdot}8H_2O$) and/or K-f zeolite ($Na_5Al_5Si_5O_{20}{\cdot}9H_2O$) (Mosbahi, 2017; Mosbahi et al., 2017).

The results of the activation process show that optimal conditions were achieved with 5% Na_2CO_3 at 75˚C for one hour. Under these conditions, the specific surface area of the raw clay increased from 30.41 m^2/g to 150 m^2/g in the activated HOA3 clay from the Oued Abiod section (**Table 2** and **Table 3**, **Figure 2**). Scanning electron microscopy (SEM) observations and XRD analyses of the Oued Abiod clays after basic activation reveal a recrystallization and complete transformation of smectitic clays into various forms of zeolites (**Figure 7(e)** and **Figure 7(f)**). These zeolites are compounds of aluminates and silicates, characterized by regular pore sizes in the nanometer range, which makes them useful as molecular sieves. These materials are widely used in catalysis, heavy oil cracking, fuel processing, and separation processes via adsorption.

The addition of sodium hydroxide during activation induces the formation of zeolites, as observed by Karsulin and Stubican (1954), Stubican (1959), and Tomita et al. (1993). The formation of Na-smectites and zeolites is closely linked to both the temperature and the pH of the synthesis (**Table 3**), as well as to the composition of the raw clay. These parameters must be precisely controlled to obtain pure Na-smectite and/or zeolites. The raw materials' content in Al^{3+} (De Kimpe, 1976; Grauby et al., 1993), Si, and Mg^{2+}, along with a high pH, favors the synthesis of zeolites. This is consistent with our results, as the clays from sample HOA3, collected from the Paleocene-Eocene boundary at Oued Abiod, are rich in Si, Al, and Mg. In contrast, for the raw clays from samples HOA1 and HOA2, which are rich in Ca^{2+} and Fe^{3+}, the basic pH seems more favorable for transforming them into sodium-rich smectites through concurrent ion substitutions: Al^{3+} by Mg^{2+} and Ca^{2+} by Na^{+}.

For the synthesis of pure smectites, Kloprogge et al. (1990) identified an optimal pH for the formation of beidellite, which ranges between 7.5 and 10. For pH values lower than 8, Iriarte et al. (2005) obtained synthetic ferriferous kaolinites, while Caillère et al. (1955) succeeded in synthesizing alumino-ferriferous smectites for pH values above 7. Therefore, the pH of fibrous clays should be carefully adjusted during their transformation into zeolites by basic activation.

6. Conclusion

The Paleocene clays from the El Haria Formation (HOA1 and HOA2) of the Oued Abiod section do not contain fibrous clays. When subjected to basic activation

with Na_2CO_3 (5%) at 75˚C for 1 hour, only partial dissolution of the dolomite occurred, along with the formation of sodium-rich smectite. In contrast, the Ypresian clays from the upper part of the section (HOA3) contain fibrous clays, such as sepiolite and palygorskite. Basic activation of these clays resulted in complete dissolution of the dolomite and the formation of well-crystallized zeolites.

Activation of these clays significantly increased their specific surface area, from 30.41 m^2/g in the raw clays to 150 m^2/g in the activated HOA3 clays. This process favored ionic exchanges (Na-Ca, Na-K, and Mg-Al) between the calcium-rich smectitic clay, dolomite, and sodium carbonate, leading to the formation of sodium-rich smectitic clays and zeolites. The basic activation of the Paleocene smectitic clays enhanced both their internal and external porosity. This porous texture, resembling sponge-like or honeycomb structures, was clearly observed by SEM.

The basic treatment, depending on the temperature, generated an alkaline environment (with a pH of 10.5), which is favorable for the partial and sometimes complete dissolution of rhombohedral dolomite and the formation of several types of zeolites with varying porosity. These sodium aluminosilicate materials are highly sought after in various industrial applications.

The formation of Na-smectites and zeolites, as detected by XRD and observed by SEM, is closely linked to the temperature, pH during synthesis, and the mineralogical and chemical composition of the raw clays. These parameters must be carefully controlled and optimized to obtain pure zeolite types. The formation of zeolites with significant porosity and both regular and irregular structures, from activated natural clays of the Paleocene-Ypresian period in the Meknassy region, presents an original and promising avenue for further research into the valorization of these clays. These zeolites exhibit pores of different sizes, including micropores (1 μm), mesopores (5 μm), macropores (10 μm), and larger macropores (greater than 10 μm).

Acknowledgements

The Paleocene-Eocene clays studied in the Meknassy region are part of the efforts to valorize Tunisian clays. We sincerely thank the team responsible for the mineralogical analysis by X-ray diffraction at the Faculty of Science of Tunis, as well as all those who contributed directly or indirectly to the completion of this work.

Conflicts of Interest

The authors declare no conflicts of interest regarding the publication of this paper.

References

Ben Ayed, N. (1986). *Evolution tectonique de l'avant pays de la chaîne alpine de la Tunisie du début du Mésozoïque à l'actuel* (328 p.). Thèse Doc. Es-sci, Université Paris-Saclay.

Boltenhagen, C. (1981). Les séquences de sédimentation du Crétacé moyen de la Tunisie centrale. In *The 1st National Congress of Earth Sciences* (p. 65).

Brindley, G. W., & Brown, G. (1980). *Crystal Structures of Clay Minerals and Their X-Ray*

Identification (pp. 197-248). Monograph 5, Mineralogical Society, London.

Caillère, S., Hénin, S., & Esquevin, J. (1955). Synthèse à basse température de quelques minéraux ferrifères (silicates et oxydes). *Bulletin de la Société française de Minéralogie et de Cristallographie, 78,* 227-241. https://doi.org/10.3406/bulmi.1955.5000

Chihi, L., Dlala, M., & Ben Ayed, N. (1984). Manifestations tectoniques synsédimentaires et polyphasées d'âge crétacé moyen dans l'Atlas tunisien central (région de Kasserine). *Comptes rendus de l'Académie des Sciences, série II, 298,* 141-146.

De Kimpe, C. R. (1976). Formation of Phyllosilicates and Zeolites from Pure Silica-Alumina Gels. *Clays and Clay Minerals, 24,* 200-207. https://doi.org/10.1346/ccmn.1976.0240408

Gamoudi, S., & Srasra, E. (2017). Characterization of Tunisian Clay Suitable for Pharmaceutical and Cosmetic Applications. *Applied Clay Science, 146,* 162-166. https://doi.org/10.1016/j.clay.2017.05.036

Gamoudi, S., & Srasra, E. (2018). Green Synthesis and Characterization of Colored Tunisian Clays: Cosmetic Applications. *Applied Clay Science, 165,* 17-21. https://doi.org/10.1016/j.clay.2018.07.042

Gougeon, R. D., Soulard, M., Miehé-Brendlé, J., Chézeau, J., Le Dred, R., Jeandet, P. et al. (2003). Analysis of Two Bentonites of Enological Interest before and after Commercial Activation by Solid Na_2CO_3. *Journal of Agricultural and Food Chemistry, 51,* 4096-4100. https://doi.org/10.1021/jf0212237

Grauby, O., Petit, S., Decarreau, A., & Baronnet, A. (1993). The Beidellite-Saponite Series: An Experimental Approach. *European Journal of Mineralogy, 5,* 623-636. https://doi.org/10.1127/ejm/5/4/0623

Iriarte, I., Petit, S., Javier Huertas, F., Fiore, S., Grauby, O., Decarreau, A. et al. (2005). Synthesis of Kaolinite with a High Level of Fe^{3+} for Al Substitution. *Clays and Clay Minerals, 53,* 1-10. https://doi.org/10.1346/ccmn.2005.0530101

Issaoui, M., Mosbahi, M., Barbieri, S., Flamini, G., Bendini, A., Ascrizzi, R. et al. (2021). Preliminary Investigation of Possible Effects of Mineral Clay Treatment Applied to Oils Produced from Olives: Focus on Moisture Removal and Compositional Changes. *Grasas y Aceites, 72,* e392. https://doi.org/10.3989/gya.1021192

Karšulin, M., & Stubičan, V. (1954). Über die Struktur und die Eigenschaften synthetischer Montmorillonite. *Monatshefte für Chemie, 85,* 343-358. https://doi.org/10.1007/bf00904000

Kloprogge, J. T., Jansen, J. B. H., & Geus, J. W. (1990). Characterization of Synthetic Na-beidellite. *Clays and Clay Minerals, 38,* 409-414. https://doi.org/10.1346/ccmn.1990.0380410

Lebedenko, F., & Plée, D. (1988). Some Considerations on the Ageing of Na_2CO_3-Activated Bentonites. *Applied Clay Science, 3,* 1-10. https://doi.org/10.1016/0169-1317(88)90002-6

Moore, D. M., & Reynolds Jr., D. C. (1997). *X-Ray Diffraction and the Identification and Analysis of Clay Minerals* (2nd ed., pp. 378-379). Oxford University Press.

Mosbahi, M. (2017). *Les argiles du Crétacé sup.—Yprésien dans la région de Meknassy-Mezzouna: Étude minéralogique, intérêt économique et apport à l'étude de l'évolution du bassin sédimentaire* (326 p.). Thèse Doc. en sciences géologiques, 3ème cycle, Univ. Sfax, Faculté des sciences de Sfax, Tunisie.

Mosbahi, M., Khlifi, M., Tlili, A., & Jamoussi, F. (2014). Influence of the Halokinesis on the Clay Mineral Repartition of Upper Maastrichtian-Ypresian in the Meknassy-Mezzouna Basin, Centerwestern Tunisia. *Arabian Journal of Geosciences, 7,* 3881-3899.

https://doi.org/10.1007/s12517-013-1050-y

Mosbahi, M., Tlili, A., Khlifi, M., & Jamoussi, F. (2017). Basic Activation of Lower Eocene Clay from Meknassy-Mezzouna Basin (Center Western Tunisia), Synthesis of Zeolite and Clarification of Soybean Oils. *Applied Clay Science, 138,* 1-11. https://doi.org/10.1016/j.clay.2016.12.011

Sdiri, A., Khairy, M., Bouaziz, S., & El-Safty, S. (2016). A Natural Clayey Adsorbent for Selective Removal of Lead from Aqueous Solutions. *Applied Clay Science, 126,* 89-97. https://doi.org/10.1016/j.clay.2016.03.003

Sheela Evangeline, Y., Vinod, S., & Manju, A. K. (2009). *Permeability Variation of Sodium Activated Bentonites. IGC 2009, Guntur, India*. Indian Geotechnical Society.

Soyer, C. (1987). *Evolution géodynamique de la direction atlasique: Exemple du Jebel Boudinar*. I.A.S, Tunisie.

Stubičan, V. (1959). Clay Mineral Research at the Institute for Silicate Chemistry, Zagreb. *Clays and Clay Minerals (National Conference on Clays and Clay Minerals), 7,* 295-302. https://doi.org/10.1346/ccmn.1958.0070120

Sylla Gueye, R., Davy, C. A., Cazaux, F., Ndiaye, A., Diop, M. B., Skoczylas, F. et al. (2017). Mineralogical and Physico-Chemical Characterization of Mbodiene Palygorskite for Pharmaceutical Applications. *Journal of African Earth Sciences, 135,* 186-203. https://doi.org/10.1016/j.jafrearsci.2017.08.019

Tomita, K., Yamane, H., & Kawano, M. (1993). Synthesis of Smectite from Volcanic Glass at Low Temperature. *Clays and Clay Minerals, 41,* 655-661. https://doi.org/10.1346/ccmn.1993.0410603

Warren, J. (2000). Dolomite: Occurrence, Evolution and Economically Important Associations. *Earth-Science Reviews, 52,* 1-81. https://doi.org/10.1016/s0012-8252(00)00022-2

Yildiz, N., & Calimli, A. (2002). Alteration of Tree Turkish Bentonites by Treatment with Na_2CO_3 and H_2SO_4. *Turkish Journal of Chemistry, 26,* 393-401.